

# A Self-Priming Digital Polymerase Chain Reaction Chip for Multiplex Genetic Analysis

Juxin Yin, Zheyu Zou, Fangfang Yin, Hongxiao Liang, Zhenming Hu, Weibo Fang, Shaowu Lv, Tao Zhang, Ben Wang, and Ying Mu\*



Cite This: *ACS Nano* 2020, 14, 10385–10393



Read Online

ACCESS |



Metrics & More



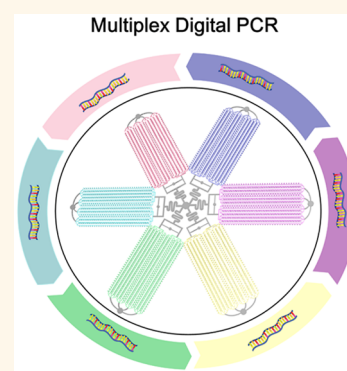
Article Recommendations



Supporting Information

**ABSTRACT:** Digital PCR (polymerase chain reaction) is a powerful and attractive tool for the quantification of nucleic acids. However, the multiplex detection capabilities of this system are limited or require expensive instrumentation and reagents, all of which can hinder multiplex detection goals. Here, we propose strategies toward solving these issues regarding digital PCR. We designed and tested a self-priming digital PCR chip containing 6-plex detection capabilities using monochrome fluorescence, which has six detection areas and four-layer structures. This strategy achieved multiplex digital detection by the use of self-priming to preintroduce the specific reaction mix to a certain detection area. This avoids competition when multiple primer pairs coexist, allowing for multiplexing in a shorter time while using less reagents and low-cost instruments. This also prevents the digital PCR chip from experiencing long sample introduction time and evaporation. For further validation, this multiplex digital PCR chip was used to detect five types of EGFR (epidermal growth factor receptor) gene mutations in 15 blood samples from lung cancer patients. We conclude that this technique can precisely quantify EGFR mutations in high-performance diagnostics. This multiplex digital detection chip is a simple and inexpensive test intended for liquid biopsies. It can be applied and used in prenatal diagnostics, the monitoring of residual disease, rapid pathogen detection, and many other procedures.

**KEYWORDS:** digital PCR, microfluidic chip, multiplex detection, self-priming, mutation



Digital polymerase chain reaction (dPCR)<sup>1,2</sup> is a precise and promising technology<sup>3</sup> that dispenses reaction solution into thousands of microwells. Each unit contains 0 or 1 template where an independent PCR reaction occurs. By counting the positive fluorescence units combined with Poisson distribution,<sup>4</sup> the number of copies of the initial template is obtained without using standard curves.<sup>5,6</sup> With the development of microfluidic technology, dPCR has been integrated for practical use.<sup>7–9</sup>

Digital PCR such as droplet digital PCR<sup>10–13</sup> (ddPCR) and chamber-based digital PCR (cdPCR) are commonly used.<sup>14–16</sup> Droplet digital PCR is a popular choice for many commercial products such as Biorad Qx and Naica crystal. Also, there are different types of ddPCR. For example, Du's group proposed a reusable ddPCR chip based on step emulsification quantitatively evaluating the HER2 gene,<sup>17</sup> and Mao's group proposed a mineral oil-saturated ddPCR chip that avoids evaporation during thermal cycling. This chip has successfully been applied for the detection of pathogens<sup>18</sup> and quantification of lung cancer-related micro-RNAs.<sup>15</sup> Compared to ddPCR, real-time detection and the more stable physical partition of cdPCR are clear advantages. Additionally, ddPCR must have control subassemblies, such as syringe pumps and air pressure,<sup>19</sup> and these are not favorable for clinical applications.<sup>5,20,21</sup> However,

even commercial instruments also are negatively impacted by these shortcomings.<sup>5</sup> Thus, the cdPCR chip was developed to facilitate the application of dPCR,<sup>20,22</sup> and many different types of these chips were proposed.<sup>23–27</sup> For example, Shen *et al.*<sup>28</sup> developed a slip chip containing 1280 wells and provided a simple quantification of nucleic acids. This group also proposed a slip chip<sup>29</sup> that has the ability to perform multiple volume digital PCR. This simultaneously detects five targets through a five separate sample introduction on a single chip. Our group also proposed a scalable self-priming fractal branching microchannel net digital PCR chip that contains 4096 microwells, and this approach does not experience sample loss.<sup>22</sup>

The rapid development of these technologies has promoted the application of digital PCR. Although digital PCR is a high-precision detection technology, its multiplex capabilities are

**Received:** May 19, 2020

**Accepted:** August 10, 2020

**Published:** August 14, 2020



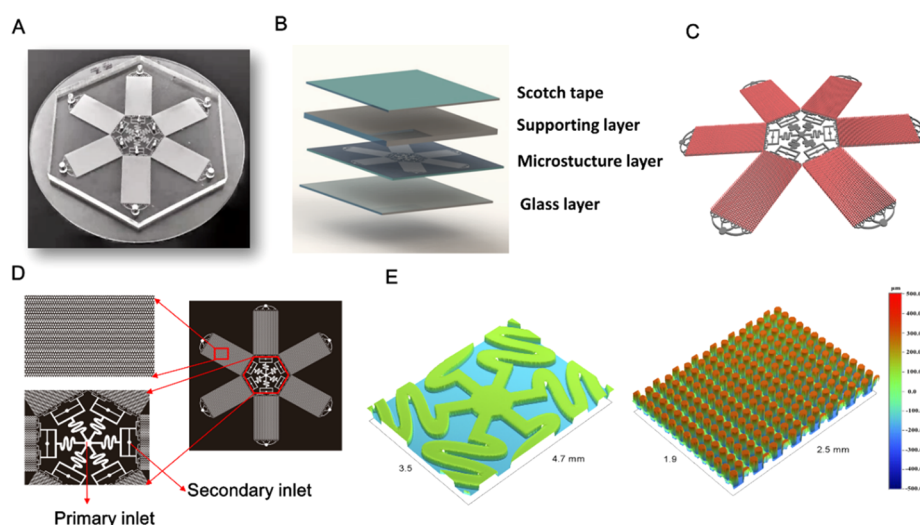


**Figure 1.** Design and structure of the multiplex digital PCR chip. (A) Photographs of the multiplex digital PCR chip. The chip was generated with PDMS (4.8 cm) and assembled using a glass slide (5 cm). (B) Detailed multilayer structures of the multiplex digital PCR chip. (C) A 3D schematic diagram of the microstructure. (D) Schematic diagram of the planar structure of the chip: the chip contains one primary inlet and six secondary inlets; the chip has six detection areas, and each area has 4800 microchambers. (E) NT9100 interference microscopy (Veeco, USA) measurement of the microstructure layer height. The heights of the microchannel and microchamber are 50 and 100  $\mu\text{m}$ , respectively.

limited. Multiplex detection saves precious samples, reduces the time to obtain results, and also reduces reagent consumption.<sup>30–32</sup> Therefore, it is important to develop multiplex detection capabilities for digital PCR.<sup>33</sup> There are two main methods where digital PCR achieves multiplex detection. First, instruments need to be equipped with multiplex fluorescent channels using multiplex fluorescent dyes to label different target genes.<sup>34–36</sup> Second, single fluorescence with different intensities must be used.<sup>31</sup> The multiple target genes in the system use the same fluorescent dyes. However, the primer concentrations of the target genes must be different. This way, intensities of fluorescence for target genes are different at the end of the amplification step. For example, Didelot *et al.*<sup>37</sup> developed a multiplex ddPCR assay to detect four different length (78, 159, 197, and 550 bp) targets. In this assay, they use combined two-color TaqMan probes (FAM and VIC) and two concentrations (0.16 and 0.2 mol/L) to identify four types of DNA fragments. Bai *et al.*<sup>38</sup> proposed a cdPCR chip to perform multiplex detection. This strategy also used different fluorescent labels for target genes and detected two types of lncRNA from extracellular vesicles. However, these two methods require a high number of fluorescent channels and instruments, which ultimately leads to high costs.<sup>33</sup> Additionally, since multiplex pairs of primers coexist, the competitive response needs to be optimized.<sup>39</sup> With this method, there will be an increase in costs that will make it necessary to develop a multiplex digital PCR chip to meet demand.

Here, we describe a powerful multiplex digital PCR chip that can simultaneously detect six target genes. This chip proposes a strategy to preintroduce specific probes and primers while overcoming current problems that multiplex dPCR faces. As proof of concept, we used this multiplex dPCR chip to quantify five types of EGFR mutations from 15 lung cancer patient samples.

## RESULTS AND DISCUSSION

**Design and Fabrication of Multiplex Digital PCR Chip.** A photograph of the multiplex digital PCR chip is portrayed in Figure 1A. This multiplex digital PCR chip measures 4.8 cm in length and consists of four layers including the glass layer, microstructure layer, support layer, and high-definition (HD) Scotch tape (Figure 1B). This chip (Figure 1C) contained six independent detection areas, and each area consisted of microchambers and microchannels. Moreover, it included one primary inlet and six independent secondary inlets (Figure 1D). The primary inlet measured 1.2 mm in diameter and was used to introduce the reaction mixture. The six secondary inlets measured 1 mm in diameter and were used to introduce the reaction mix that contained specific primers and probes. There were 4800 microchambers in each individual area, with a total of 28 800 microchambers in six. The planar shape of the microchambers was circular with a diameter of 100  $\mu\text{m}$ . The depth-to-width ratio of the microchambers was 1:1. Also, we can flexibly process by changing the number of microchambers according to the detection requirements (Table S1). The curve in the middle of the chip is designed to prevent the cross-contamination of primers and probes in different areas, which had a height of 50  $\mu\text{m}$  (Figure 1E).

The multiplex chip is a self-priming and dispensing digital PCR chip based on polydimethylsiloxane (PDMS). Compared to other digital PCR chips,<sup>22</sup> the most significant advantage of this chip is its flexibility in defining the number (1–6) of detection targets, which is for researchers to get enough information from one time experiment. In addition, our approach for multiplex detection is to preintroduce primers of different target genes into six independent detection areas. This method not only avoids competitive reactions when multiple primer pairs coexist but also reduces time and reagent-related costs. Moreover, only one kind of fluorescent probe can be used to achieve up to 6-fold detection, which reduces costs in reagents and instruments.

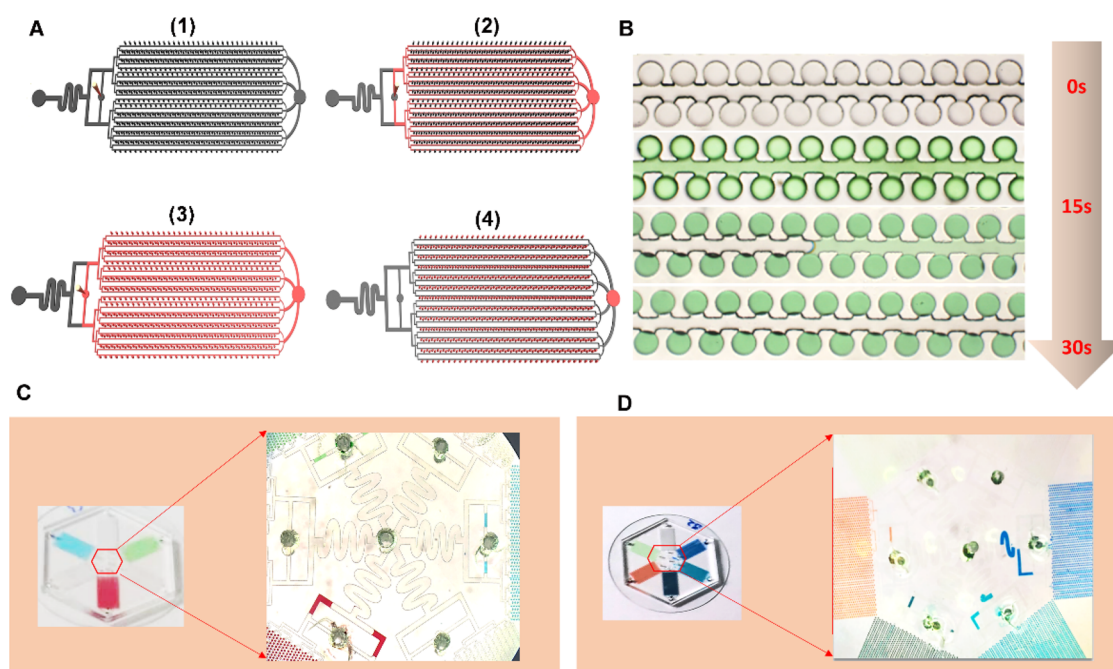


**Figure 2.** Preintroduction of a reaction mix into each detection area. (A) Schematic diagram of pre-embedding. (1) Opening of the primary and secondary inlets. Insertion of the pipet tip containing the mix solution into the secondary inlet. (2) Under negative pressure, mixed liquid from the secondary inlet enters the channel. As a result of air entering the chip, the mix will not enter other areas. (3) The mix solution fills the microchannel and all the microchambers. (4) Air enters into the channel, separating each reaction chamber, while waste liquid enters the waste liquid port. When the process is completed, the secondary inlet is blocked with a curing agent (5:1 PDMS with 10  $\mu\text{L}$  of platinum catalyst). (B) Photographs of the preintroduction process. These photographs correspond to (1)–(4) of Figure 2A. (C) Preintroduction of three-color dyes. (D) Preintroduction of five color dyes.

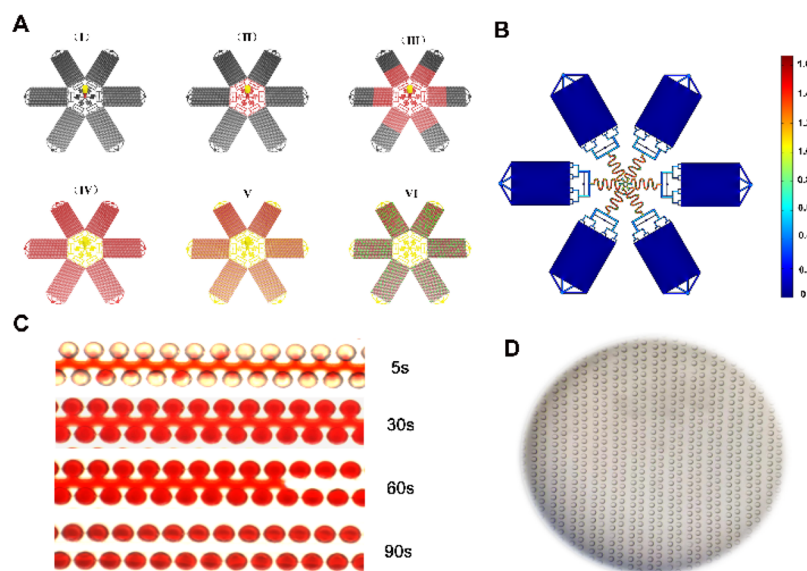


**Figure 3.** Sample introduction of multiplex digital PCR chip. (A) Diagram of self-priming of the multiplex digital PCR chip. (I) The chip is under negative pressure, the tip contains the oil phase, and sample is inserted into the primary inlet. (II) The reaction solution enters all areas along the microchannel at a uniform speed. (III) The reaction solution arrives into the detection area. (IV) The PDMS oil phase comes into the chip. (V) The PDMS oil phase separates each microchamber. (VI) After the digital PCR reaction, the fluorescent signal can be observed. (B) Theoretical predictions of the flow velocity in the microchannels entering the six detection areas are consistent. (C) Photographs of the self-priming process. Compared to the photo in Figure 2B, after the PDMS oil enters the channel, the channel is not visible under the microscope. (D) Photograph of the microchamber in the chip after the self-priming process. Each independent chamber was observed.

### Principle for Pre-embedding Primers and Probes.

One challenging task faced by multiplex digital PCR chips is a method of introducing different types of primers and probes into specific regions while avoiding cross-contamination.

Previous methods added primers and probes to a characteristic area manually or using robotics. These methods are not suitable for digital PCR chips because the diameter of the microchamber is too small. To achieve separation, pumps and

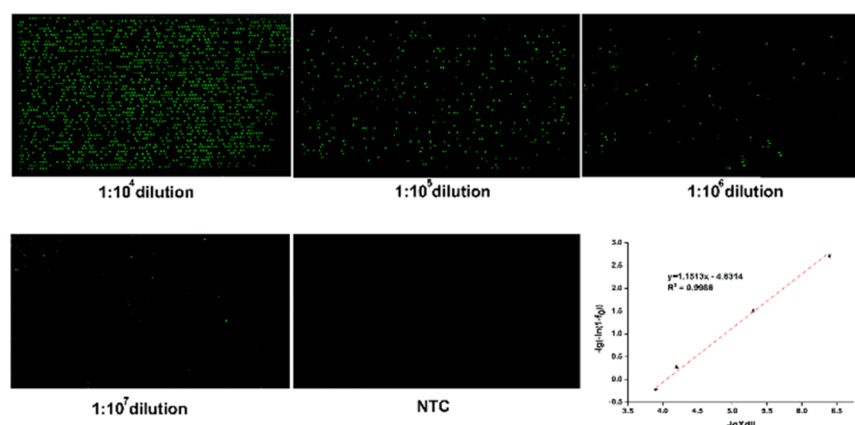


**Figure 4.** Quantitative performance of digital PCR. Fluorescent images of the digital PCR for a serial dilution of a human ACTB plasmid. NTC refers to no template control. Data were expressed as means, and all experiments were done in triplicate. The linear regression curve was obtained by plotting  $-\log(-\ln(1 - f_0))$  against  $-\log X_{dil}$ .

valves can be used. This increases the complexity of operation and the reagent waste and leads to uneven distribution, all of which are not suitable for practical application. Therefore, a method to introduce primers and probes to specific areas needs to be developed.

To solve this issue, we introduced a mix (PCR reaction buffer, specific primers and probe, trehalose) into the chip based on self-priming separation. The primary inlet was used as the “air pump”, and the curved design guaranteed that specific primers and probes would remain in specified areas to prevent potential cross-contamination. First, the primary and secondary inlets should be opened (Figure 2A). Next, the specific mix should be introduced into the tip, and the tip should then be inserted into a secondary inlet. Under negative pressure, the primer and probe mix will enter the microchambers and be separated by air. Due to the curved design and the primary inlet being open, the reagents will stay in their specific area and minimize cross-contamination.

Comsol software was used to simulate liquid motion (Figure S3) to confirm the feasibility of this method. Results from the theoretical simulation reveal that liquid does not flow into the central channel, which indicates that specific primers and probes will only be introduced into separate areas. Using this method, specific primers and probes can be embedded into independent microchambers within 30 s (Figure 2B). To further validate, we used three and five different dyes to embed into specific areas (Figure 2C and D). Data show that different color dyes remained in specific areas.

In order to make multiplex dPCR more suitable for clinical applications, the mix was freeze-dried in the chip and trehalose was added as the excipient for long-term 4 °C storage. As described in Figure S4, the chip can be stored in lyophilized form at 4 °C for at least 60 days. This way, a user only needs to introduce the sample solution into the chip when performing multiplex detection, which reduces manual operation time and increases practicability.

**Sample Loading.** To reduce complexity and reliance on pumps, we took advantage of PDMS air permeability and used negative pressure as a power source to perform equipment-free loading and automatic sample compartmentalization. As illustrated in Figure 3A, the sample solution is first inserted into the chip followed by PDMS oil entering the channel to separate the microchambers. After performing the digital PCR reaction, positive microchambers were observed.

The principle of self-priming liquid separation has been previously reported.<sup>40</sup> In order to ensure the sample remained in the microchambers and prevent cross-contamination, this technology generally uses a thermo-curing PDMS oil. Due to the high viscosity of this oil and the long distance it travels, there is a significant increase in loading time. This problem can be easily neglected. For example, Yeh *et al.* proposed a vacuum battery on the chip where loading time needs 10 min to separate 224 microchambers.<sup>41</sup> The digital PCR chip<sup>22</sup> proposed by our previous work only needs 20 min to separate 4096 microchambers. By reducing the loading time, it is possible to make a chip more favorable for point-of-care and other applications.

For this multiplex digital PCR chip, we have used a radial design so that each independent area does not influence one another, when using the self-priming principle (Figure 3A). Each independent area had 48 branch channels, and the length of the independent areas was only 2 cm, which shortened the distance. First, theoretical simulation (Figure 3B) revealed that the speeds of the six regions were consistent when the sample was loaded. We also provided a supplemental video that further demonstrates that speeds were almost consistent in the six regions. As shown in Figure 3C and D, all 28 800 microchambers are quickly filled with reaction solution and separated by PDMS oil in 90 s. This chip can achieve fast sample loading.

**Real-Time Quantitative and Multiplex Performance of Digital PCR Chips.** The ACTB gene was used to detect the quantitative performance of digital PCR chips. The multiplex chip can be used to analyze a single sample at a dynamic range of 4 orders of magnitude (6-plex) to 5 orders of magnitude (1-plex). We have tested the 10-fold dilutions of the plasmid stock DNA ranging from 1:10<sup>4</sup> to 1:10<sup>7</sup>. The fluorescent image of digital PCR is shown in Figure 4. These results were calibrated using Poisson distribution. As shown in Supporting Information S6, there was a linear relationship between  $-\log(-\ln(1 - f_0))$  and  $-\log X_{dil}$ . We obtained a linear fitting curve  $y = 1.513x - 4.6314$  ( $R^2 = 0.9986$ ), and then the concentration was calculated to be  $2.05 \times 10^8$  copies/ $\mu$ L. This result was consistent with measurements obtained by Qubit 3.0.

Digital PCR is a technique that relies on end-point detection. Compared to end-point detection, real-time fluorescence detection for dPCR can be an alternative method

that improves quantitative accuracy.<sup>9,42,43</sup> Since this chip possesses a fixed array, it can also be used for real-time signal detection. We performed real-time dPCR where fluorescence images were captured every five cycles from cycle 10 to 45. As shown in Figure 5, a false positive fluorescent spot was

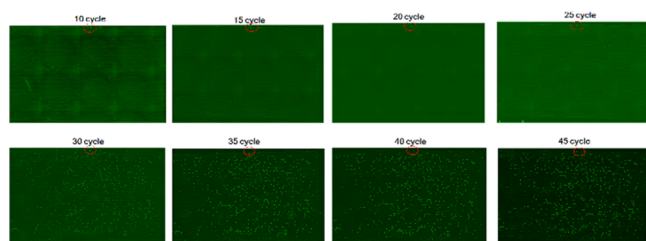


**Figure 5.** Real-time dPCR results using this self-priming dPCR chip. Fluorescence images were captured every five cycles from cycle 10 to 45. By capturing the fluorescence image in real time, we can exclude false positive amplification and thus obtain a more accurate concentration.

identified in the fluorescent image of the 10th cycle. Through this real-time detection, we could eliminate this bright spot and make the quantitative results more accurate. Also, by simulating the fluorescence change curve at a certain point (Figure S6), we distinguished true and false positives through fluorescence change.

We used five types of EGFR mutations to verify multiplex detection performance (Figure 6). The commercial Biorad-Qx200 digital PCR system was also used to test these results. Since the current multiplex system needs to be optimized and the 1-plex result of Qx200 is more reliable, we compare the results with Qx200 1-plex. As shown in Figure S7, there were no significant differences ( $P > 0.05$ ) between the digital PCR chip and the commercial platform for EGFR mutations.

Although many commercial companies have introduced premisses for multiplex digital PCR, these can be quite expensive. In addition, the instrument needs to be equipped with multiple fluorescent channels. These issues will increase

costs and especially become a burden for patients in clinical settings. Here, only ordinary PCR mix and one fluorescence channel are required to achieve multiplex detection using our proposed digital PCR chip.

**Liquid Biopsy of Lung Cancer Patients Using This Multiplex dPCR Chip in Tested Patients.** Lung cancer is the leading cause of cancer death worldwide,<sup>44</sup> where non-small-cell lung cancer (NSCLC) accounts for approximately 80% of all lung cancer cases.<sup>45</sup> Tyrosine kinase inhibitors (TKIs) are effective drugs for EGFR-activating mutations, and they have been approved for the treatment of NSCLC.<sup>46</sup> EGFR exon 19 Del and L858R substitutions account for 85% to 90% of NSCLC cases, and first-generation TKIs such as gefitinib, erlotinib and ectinib are used for treatment.<sup>47</sup> Except for 19Del and L858R, other site mutations such as G719A and L861Q are rare mutant alleles.<sup>48</sup> For these subtypes, treatment with first-generation TKIs is not effective, and the drugs afatinib and oxitinib are better options for these specific mutations instead. In addition, approximately 60% of acquired resistance is due to a secondary mutation in the exon 20 EGFR T790M.<sup>49</sup> Currently, the only effective drug for this mutation is the third-generation TKI oxitinib. For different lung cancer patients, it is necessary to screen multiple EGFR mutant alleles to obtain a personalized and effective treatment plan.

As a proof of concept, we detected EGFR mutant alleles to prove the multiplex detection ability of this chip. We collected blood samples from lung cancer patients undergoing a liquid biopsy. We extracted ctDNA from blood samples and detected EGFR mutant alleles using a multiplex dPCR chip. It was demonstrated that our chip was able to detect the five types of EGFR mutations (Figure 6). As the defining characteristic of an assay, the limit of blank (LOB) is three copies for T790M and one copy for G719A, and no positive signal was detected for 19DEL, L858R, and L861Q. Results were considered negative when the number of fluorescence signals was less than the LOB and positive when the detection area yielded over 10 copies. Patient characteristics are listed in Table S2. As shown in Figure 7, all 15 samples were diagnosed as different NSCLC types. The L858R mutation (53.3%) was detected in eight

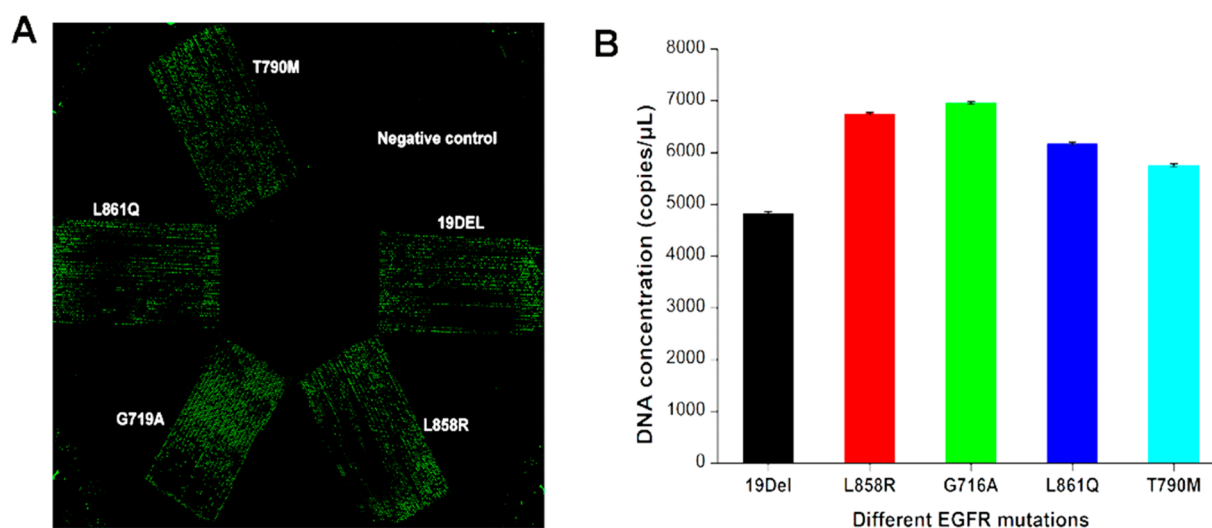


**Figure 6.** Detection of a 5-plex using this multiplex digital PCR chip. (A) Representative images obtained by detecting five mutations (L858R, G719A, 19Del, L861Q, T790M) in the EGFR gene. The image is obtained by the splicing function of the microscope. (B) Detection results of EGFR mutations after calibration. Data were expressed as mean  $\pm$  standard deviation, and all experiments were performed in triplicate.

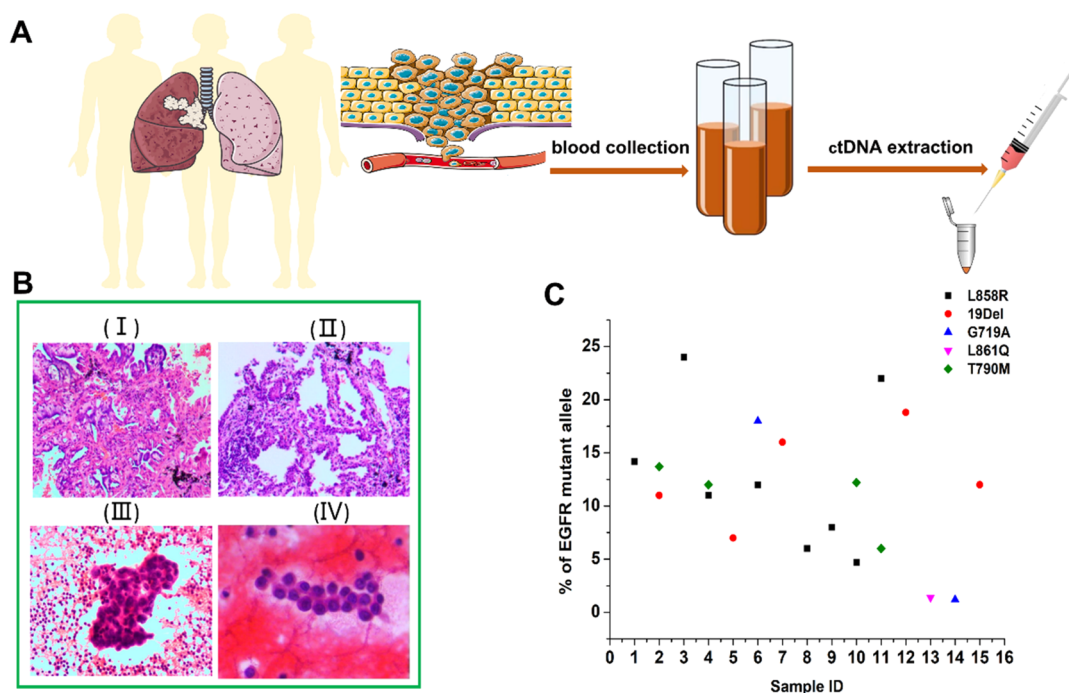


**Figure 7.** Pathological section and liquid biopsy of NSCLC cases. (A) Schematic of sample preparation process for liquid biopsies. (B) Representative tissue sections of patients with different types of NSCLC. (I) Invasive adenocarcinoma, (II) adenocarcinoma *in situ*, (III) adenocarcinoma cells from hydrothorax, (IV) adenocarcinoma cells from lymph node puncture fluid. (C) Content of five mutant genes (L858R, G719A, 19Del, L861Q, T790M) obtained by the multiplex digital PCR chip consisting of samples from 15 patients. Data were expressed as means, and all experiments were performed in triplicate. All patients have EGFR mutations, and results are reported as % EGFR mutant allele.

patients (stage II–IV), ranging from 4.7% to 24%. T790M was identified in three patients (one in stage II, two in stage III) with a range from 6% to 12.2%. Only one patient (case 6) in stage III carried both L858R and G719A mutations. The 19 Del mutation (40%) was found in five patients with a range from 7% to 18.4%. Among them, one patient (case 2) in stage II was detected to have the T790M mutation with 13.7%. Case 14 (6%) in stage III had the G719A mutation (1.2%). One patient in stage II had the L861Q mutation (1.4%). Digital PCR was capable of detecting EGFR mutations.<sup>44,50,51</sup> This self-priming monochrome fluorescence multiplex dPCR chip was also successfully applied to the detection of EGFR mutant alleles, and more detailed information about EGFR mutations can be found in patients using this multiplex dPCR chip. Therefore, a personalized plan can be developed for each patient.

## CONCLUSIONS

Motivated by current multiplex digital PCR issues in point-of-care clinical applications, we successfully develop a multiplex digital PCR chip and tested its applicability in a clinical context. The feasibility of establishing a strategy for pre-embedding a reaction mix and achieving multiplex detection have been demonstrated. This strategy agreed with the previous theoretical predictions. Also, this multiplex chip has high sensitivity and real-time quantitative capacity. Moreover, fast-track implementation for sample introduction makes this chip robust and practical. This chip can simultaneously detect six types of targets, and its capacity of collecting information on multiple targets in one injection can provide more information to researchers and enhance practical applications.

At the same time, this multiplex chip can be used for digital PCR and isothermal nucleic acid detection. If we apply the isothermal amplification techniques such as recombinase polymerase amplification (RPA)<sup>52–55</sup> and loop-mediated isothermal amplification (LAMP)<sup>56–59</sup> on this multiplex chip, it will be much more valuable for pathogen detection, environmental monitoring, and more.

## METHODS

**Reagents.** Polydimethylsiloxane was purchased from GE Advanced Materials (USA). SU8 3000 series negative photoresist was obtained from MicroChem. Trimethylchlorosilane was purchased from Sigma-Aldrich (USA), and Parylene C was purchased from Special Coating System (USA). EGC-1720 was obtained from 3M (USA), and HD Scotch tape was purchased from Duck (USA). Lastly, the QIAamp circulating nucleic acid kit was purchased from Qiagen (USA). The primers and probes for EGFR mutation were purchased from RainSure Scientific (China) and Thermo Fisher Scientific (USA). Sequences were protected by these companies. PCR mix was purchased from Thermo Fisher Scientific (USA).

### Design and Fabrication of the Multiplex Digital PCR Chip.

The image was designed by Coreldraw X7, and the mask was printed using a 5000 dpi printer. The mold was processed through standard multilayer soft lithography by first making a microchannel and then a microchamber. First, the silicon wafer was cleaned and heated at 200 °C for 10 min to completely remove surface moisture. Next, a 50 μm thick photoresist (SU8-3050) was coated on the silicon wafer using a spin coater. The coated silicon wafer was placed on a program-controlled temperature plate, heated for 15 min at 95 °C for 15 min, and cooled at room temperature. The mask was attached to a quartz glass plate, and the silicon wafer was exposed for 10 s using a UV exposure machine (8 mJ/cm<sup>2</sup>). The exposed silicon wafer was heated on a programmed temperature-controlled plate at 65 °C for 1 min and 95 °C for 5 min and cooled at room temperature. Afterward, fabrication of the microchamber layer was performed. A 50 μm thick

photoresist layer was coated on the silicon wafer, and the subsequent operating procedures are consistent with the manufacture of the microchannel layer. The UV exposure time was adjusted to 10 s. Finally, the silicon wafer was developed and baked at 200 °C for 30 min.

The chip was composed of PDMS and glass. The mold was first treated with trimethylchlorosilane for 5 min. A total of 5 g of PDMS (A:B/S:1) was poured onto the mold and evenly spread using a spin coater. The program was rotated at 500 rpm for 10 s and then 1000 rpm for 30 s. After heating at 85 °C for 5 min, 1 mL of EGC-1720 was spin-coated on top of the PDMS layer to form a 10 nm thick layer that contained low permeability. Next, 23 g of PDMS (A:B/10:1) was poured onto the mold and heated at 85 °C for 30 min. Finally, the chip was bound with glass after plasma treatment.

**Multiplex Digital PCR Chip Operation.** First, a layer of HD Scotch tape was placed on the surface of the chip to prevent air leakage. The chip was placed in a vacuum tank and degassed to 0.1 kPa for 20 min. Meanwhile, primer and probe mixes for different target genes were prepared. The primary and secondary inlets were broken in sequence by the needle. The pipet tip was inserted into the secondary inlet. Next, a mixture of PDMS (10:1) and Pt catalyst (10  $\mu$ L) was injected into the secondary inlet to seal it. Based on detection requirements, specific primers and probes for different target genes could be introduced into six different regions. HD Scotch tape was placed on the chip before lyophilization. The primer and probe mix in the chip were then lyophilized for 1 h.

As a result of lyophilization, the chip was in a negative pressure state, and the sample introduction process was able to be directly completed. First, the reaction systems, except for the probe and primers, were prepared and introduced into the pipet tip. The pipet tip was inserted into the primary inlet, and mineral oil was added. The reaction buffer and mineral oil were introduced into the chip in a self-priming way, and the whole process was completed quickly in only 90 s.

**Digital PCR Reaction.** All digital PCR experiments followed the MIQE guidelines for dPCR.<sup>60</sup> The mix used for lyophilization included 2.5  $\mu$ L of PCR mix, 150 nM primers and probe mix, and 5% trehalose. The sample solution consisted of RNase-free H<sub>2</sub>O, template DNA, and 1.5  $\mu$ L of 0.2% Tween-20. The PCR process was as follows: 50 °C for 2 min, 95 °C for 10 min, 15 s at 95 °C, and 1 min at 60 °C, for 40 cycles.

**Multiplex Detection of the EGFR Mutations.** For each patient, 10 mL of blood was collected. Whole blood was centrifuged at 1300g for 5 min at 4 °C. The upper layer of plasma was removed and transferred into a 1.5 mL centrifuge tube, and 4–5 mL of plasma was isolated. A 2 mL amount of plasma was used to perform ctDNA extraction. The ctDNA was extracted following procedures provided by the QIAamp circulating nucleic acid kit. The 15 cases were simultaneously analyzed for 19Del, L858R, G719A, L861Q, and T790 M and a positive control (wild type, WT) in this multiplex chip. The negative control is the addition of RNase-free H<sub>2</sub>O to another chip. All results were reported as percent of EGFR mutant alleles.

**Imaging and Data Analyses.** On-chip results were detected using fluorescence microscopy (USA). The fluorescent signals of the probes were labeled with FAM. The excitation light was measured at a wavelength of 455 nm, while a 495 nm long-pass filter received the emitted light through a CCD camera.

## ASSOCIATED CONTENT

### Supporting Information

The Supporting Information is available free of charge at <https://pubs.acs.org/doi/10.1021/acsnano.0c04177>.

Processing flow of digital PCR chip, optimal number of different sized microchambers, high uniformity of the digital chip PCR, theoretical simulation of liquid motion, storage time of lyophilized ingredients, antievaporation test, Poisson distribution for data calibration, real-time

detection, quantitative results of commercial platform, result of positive control, patient characteristics (PDF) (MP4)

## AUTHOR INFORMATION

### Corresponding Author

**Ying Mu** – Research Centre for Analytical Instrumentation, Institute of Cyber-Systems and Control, State Key Laboratory of Industrial Control Technology, Zhejiang University, Hangzhou, Zhejiang Province 310058, China; [orcid.org/0000-0002-4322-2522](https://orcid.org/0000-0002-4322-2522); Email: [muying@zju.edu.cn](mailto:muying@zju.edu.cn)

### Authors

**Juxin Yin** – Research Centre for Analytical Instrumentation, Institute of Cyber-Systems and Control, State Key Laboratory of Industrial Control Technology, Zhejiang University, Hangzhou, Zhejiang Province 310058, China

**Zheyu Zou** – College of Life Sciences, Zhejiang University, Hangzhou 310058, Zhejiang, China

**Fangfang Yin** – Weifang People's Hospital, Weifang 261000, China

**Hongxiao Liang** – Research Centre for Analytical Instrumentation, Institute of Cyber-Systems and Control, State Key Laboratory of Industrial Control Technology, Zhejiang University, Hangzhou, Zhejiang Province 310058, China

**Zhenming Hu** – Research Centre for Analytical Instrumentation, Institute of Cyber-Systems and Control, State Key Laboratory of Industrial Control Technology, Zhejiang University, Hangzhou, Zhejiang Province 310058, China

**Weibo Fang** – Research Centre for Analytical Instrumentation, Institute of Cyber-Systems and Control, State Key Laboratory of Industrial Control Technology, Zhejiang University, Hangzhou, Zhejiang Province 310058, China

**Shaowu Lv** – Key Laboratory for Molecular Enzymology and Engineering of the Ministry of Education, College of Life Science, Jilin University, Changchun 130000, China

**Tao Zhang** – Research Centre for Analytical Instrumentation, Institute of Cyber-Systems and Control, State Key Laboratory of Industrial Control Technology, Zhejiang University, Hangzhou, Zhejiang Province 310058, China; [orcid.org/0000-0003-3782-0478](https://orcid.org/0000-0003-3782-0478)

**Ben Wang** – Cancer Institute (Key Laboratory of Cancer Prevention and Intervention, National Ministry of Education), The Second Affiliated Hospital, School of Medicine and Institute of Translational Medicine, Zhejiang University, Hangzhou 310009, China; [orcid.org/0000-0002-4134-1835](https://orcid.org/0000-0002-4134-1835)

Complete contact information is available at: <https://pubs.acs.org/doi/10.1021/acsnano.0c04177>

### Author Contributions

J. Yin, S. Lv, T. Zhang, B. Wang, and Y. Mu designed the experiments; J. Yin, Z. Zou, F. Yin, Z. Hu, and H. Liang performed the experiments; J. Yin, B. Wang, and Y. Mu wrote the paper. All authors have given approval to the final version of the manuscript.

### Notes

The authors declare no competing financial interest.

## ACKNOWLEDGMENTS

The authors are grateful for the financial support from the National Program on Key Research Project of China (2019YFE0103900) as well as European Union's Horizon

2020 Research and Innovation Programme under Grant Agreement No. 861917–SAFFI, the National Key R&D Program of China (2018YFF01012100), and the Fundamental Research Funds for the Zhejiang Provincial Colleges & Universities (2019XZZX003-08).

## REFERENCES

- (1) Sykes, P. J.; Neoh, S. H.; Brisco, M. J.; Hughes, E.; Condon, J.; Morley, A. A. Quantitation of Targets for PCR by Use of Limiting Dilution. *BioTechniques* **1992**, *13*, 444–449.
- (2) Vogelstein, B.; Kinzler, K. W. Digital PCR. *Proc. Natl. Acad. Sci. U. S. A.* **1999**, *96*, 9236–9241.
- (3) Heyries, K. A.; Tropini, C.; Vaninsberghe, M.; Doolin, C.; Petriv, I.; Singhal, A.; Leung, K.; Hughesman, C. B.; Hansen, C. L. Megapixel Digital PCR. *Nat. Methods* **2011**, *8*, 649–U64.
- (4) Hatch, A. C.; Fisher, J. S.; Tovarr, A. R.; Hsieh, A. T.; Lin, R.; Pentoney, S. L.; Yang, D. L.; Lee, A. P. 1-Million Droplet Array with Wide-Field Fluorescence Imaging for Digital PCR. *Lab Chip* **2011**, *11*, 3838–3845.
- (5) Sreejith, K. R.; Ooi, C. H.; Jin, J.; Dao, D. V.; Nguyen, N. T. Digital Polymerase Chain Reaction Technology - Recent Advances and Future Perspectives. *Lab Chip* **2018**, *18*, 3717–3732.
- (6) Pohl, G.; Shih Ie, M. Principle and Applications of Digital PCR. *Expert Rev. Mol. Diagn.* **2004**, *4*, 41–7.
- (7) Tadmor, A. D.; Ottesen, E. A.; Leadbetter, J. R.; Phillips, R. Probing Individual Environmental Bacteria for Viruses by Using Microfluidic Digital PCR. *Science* **2011**, *333*, 58–62.
- (8) Hindson, C. M.; Chevillet, J. R.; Briggs, H. A.; Galichotte, E. N.; Ruf, I. K.; Hindson, B. J.; Vessella, R. L.; Tewari, M. Absolute Quantification by Droplet Digital PCR Versus Analog Real-Time PCR. *Nat. Methods* **2013**, *10*, 1003.
- (9) Baker, M. Digital PCR Hits Its Stride. *Nat. Methods* **2012**, *9*, 541–544.
- (10) Schuler, F.; Trotter, M.; Geltman, M.; Schwemmer, F.; Wadle, S.; Dominguez-Garrido, E.; Lopez, M.; Cervera-Acedo, C.; Santibanez, P.; von Stetten, F.; Zengerle, R.; Paust, N. Digital Droplet PCR on Disk. *Lab Chip* **2016**, *16*, 208–216.
- (11) Chen, J.; Luo, Z.; Li, L.; He, J.; Li, L.; Zhu, J.; Wu, P.; He, L. Capillary-Based Integrated Digital PCR in Picoliter Droplets. *Lab Chip* **2018**, *18*, 412–421.
- (12) Zhang, Y.; Jiang, H. R. A Review on Continuous-Flow Microfluidic PCR in Droplets: Advances, Challenges and Future. *Anal. Chim. Acta* **2016**, *914*, 7–16.
- (13) Yen, G. S.; Fujimoto, B. S.; Schneider, T.; Kreutz, J. E.; Chiu, D. T. Statistical Analysis of Nonuniform Volume Distributions for Droplet-Based Digital PCR Assays. *J. Am. Chem. Soc.* **2019**, *141*, 1515–1525.
- (14) Quan, P. L.; Sauzade, M.; Brouzes, E. dPCR: A Technology Review. *Sensors* **2018**, *18*, 1271.
- (15) Wang, P.; Jing, F.; Li, G.; Wu, Z.; Cheng, Z.; Zhang, J.; Zhang, H.; Jia, C.; Jin, Q.; Mao, H. Absolute Quantification of Lung Cancer Related MicroRNA by Droplet Digital PCR. *Biosens. Bioelectron.* **2015**, *74*, 836–842.
- (16) Basha, I. H. K.; Ho, E. T.; Yousuff, C. M.; Bin Hamid, N. H. Towards Multiplex Molecular Diagnosis-A Review of Microfluidic Genomics Technologies. *Micromachines* **2017**, *8*, 266.
- (17) Nie, M.; Zheng, M.; Li, C.; Shen, F.; Liu, M.; Luo, H.; Song, X.; Lan, Y.; Pan, J. Z.; Du, W. Assembled Step Emulsification Device for Multiplex Droplet Digital Polymerase Chain Reaction. *Anal. Chem.* **2019**, *91*, 1779–1784.
- (18) Bian, X.; Jing, F.; Li, G.; Fan, X.; Jia, C.; Zhou, H.; Jin, Q.; Zhao, J. A Microfluidic Droplet Digital PCR for Simultaneous Detection of Pathogenic *Escherichia Coli* O157 and *Listeria Monocytogenes*. *Biosens. Bioelectron.* **2015**, *74*, 770–777.
- (19) Beer, N. R.; Hindson, B. J.; Wheeler, E. K.; Hall, S. B.; Rose, K. A.; Kennedy, I. M.; Colston, B. W. On-Chip, Real-Time, Single-Copy Polymerase Chain Reaction in Picoliter Droplets. *Anal. Chem.* **2007**, *79*, 8471–8475.
- (20) Heyries, K. A.; Tropini, C.; Vaninsberghe, M.; Doolin, C.; Petriv, O. I.; Singhal, A.; Leung, K.; Hughesman, C. B.; Hansen, C. L. Megapixel Digital PCR. *Nat. Methods* **2011**, *8*, 649–651.
- (21) Witters, D.; Sun, B.; Begolo, S.; Rodriguez-Manzano, J.; Robles, W.; Ismagilov, R. F. Digital Biology and Chemistry. *Lab Chip* **2014**, *14*, 3225–3232.
- (22) Zhu, Q.; Xu, Y.; Qiu, L.; Ma, C.; Yu, B.; Song, Q.; Jin, W.; Jin, Q.; Liu, J.; Mu, Y. A Scalable Self-Priming Fractal Branching Microchannel Net Chip for Digital PCR. *Lab Chip* **2017**, *17*, 1655–1665.
- (23) Cohen, D. E.; Schneider, T.; Wang, M.; Chiu, D. T. Self-Digitization of Sample Volumes. *Anal. Chem.* **2010**, *82*, 5707–5717.
- (24) Tian, Q.; Yu, B.; Mu, Y.; Xu, Y.; Ma, C.; Zhang, T.; Jin, W.; Jin, Q. An Integrated Temporary Negative Pressure Assisted Microfluidic Chip for DNA Isolation and Digital PCR Detection. *RSC Adv.* **2015**, *5*, 81889–81896.
- (25) Thompson, A. M.; Gansen, A.; Paguirigan, A. L.; Kreutz, J. E.; Radich, J. P.; Chiu, D. T. Self-Digitization Microfluidic Chip for Absolute Quantification of mRNA in Single Cells. *Anal. Chem.* **2014**, *86*, 12308–12314.
- (26) Wang, Y. Z.; Southard, K. M.; Zeng, Y. Digital PCR Using Micropatterned Superporous Absorbent Array Chips. *Analyst* **2016**, *141*, 3821–3831.
- (27) Yin, J.; Hu, J.; Sun, J.; Wang, B.; Mu, Y. A Fast Nucleic Acid Extraction System for Point-of-Care and Integration of Digital PCR. *Analyst* **2019**, *144*, 7032–7040.
- (28) Shen, F.; Du, W. B.; Kreutz, J. E.; Fok, A.; Ismagilov, R. F. Digital PCR on a SlipChip. *Lab Chip* **2010**, *10*, 2666–2672.
- (29) Shen, F.; Sun, B.; Kreutz, J. E.; Davydova, E. K.; Du, W. B.; Reddy, P. L.; Joseph, L. J.; Ismagilov, R. F. Multiplexed Quantification of Nucleic Acids with Large Dynamic Range Using Multivolume Digital RT-PCR on a Rotational SlipChip Tested with HIV and Hepatitis C Viral Load. *J. Am. Chem. Soc.* **2011**, *133*, 17705–17712.
- (30) Vannitamby, A.; Hendry, S.; Irving, L.; Steinfert, D.; Bozinovski, S. Novel Multiplex Droplet Digital PCR Assay for Scoring PD-L1 in Non-Small Cell Lung Cancer Biopsy Specimens. *Lung Cancer* **2019**, *134*, 233–237.
- (31) Zhong, Q.; Bhattacharya, S.; Kotsopoulos, S.; Olson, J.; Taly, V.; Griffiths, A. D.; Link, D. R.; Larson, J. W. Multiplex Digital PCR: Breaking the One Target Per Color Barrier of Quantitative PCR. *Lab Chip* **2011**, *11*, 2167–2174.
- (32) Shen, F.; Du, W. B.; Davydova, E. K.; Karymov, M. A.; Pandey, J.; Ismagilov, R. F. Nanoliter Multiplex PCR Arrays on a SlipChip. *Anal. Chem.* **2010**, *82*, 4606–4612.
- (33) Denis, J. A.; Guillerme, E.; Coulet, F.; Larsen, A. K.; Lacorte, J. M. The Role of BEAMing and Digital PCR for Multiplexed Analysis in Molecular Oncology in the Era of Next-Generation Sequencing. *Mol. Diagn. Ther.* **2017**, *21*, 587–600.
- (34) Chen, W.; Zheng, J.; Wu, C.; Liu, S.; Chen, Y.; Liu, X.; Du, J.; Wang, J. Breast Cancer Subtype Classification Using 4-Plex Droplet Digital PCR. *Clin. Chem.* **2019**, *65*, 1051–1059.
- (35) Zonta, E.; Garlan, F.; Pecuchet, N.; Perez-Toralla, K.; Caen, O.; Milbury, C.; Didelot, A.; Fabre, E.; Blons, H.; Laurent-Puig, P.; Taly, V. Multiplex Detection of Rare Mutations by Picoliter Droplet Based Digital PCR: Sensitivity and Specificity Considerations. *PLoS One* **2016**, *11*, No. e0159094.
- (36) Ottesen, E. A.; Hong, J. W.; Quake, S. R.; Leadbetter, J. R. Microfluidic Digital PCR Enables Multigene Analysis of Individual Environmental Bacteria. *Science* **2006**, *314*, 1464–1467.
- (37) Didelot, A.; Kotsopoulos, S. K.; Lupo, A.; Pekin, D.; Li, X. Y.; Atochin, I.; Srinivasan, P.; Zhong, Q.; Olson, J.; Link, D. R.; Laurent-Puig, P.; Blons, H.; Hutchison, J. B.; Taly, V. Multiplex Picoliter-Droplet Digital PCR for Quantitative Assessment of DNA Integrity in Clinical Samples. *Clin. Chem.* **2013**, *59*, 815–823.
- (38) Bai, Y. A.; Qu, Y. L.; Wu, Z. H.; Ren, Y. J.; Cheng, Z. L.; Lu, Y. X.; Hu, J.; Lou, J. T.; Zhao, J. L.; Chen, C.; Mao, H. J. Absolute Quantification and Analysis of Extracellular Vesicle lncRNAs from the Peripheral Blood of Patients with Lung Cancer Based on Multi-

Colour Fluorescence Chip-Based Digital PCR. *Biosens. Bioelectron.* **2019**, *142*, 111523.

(39) Quick, J.; Grubaugh, N. D.; Pullan, S. T.; Claro, I. M.; Smith, A. D.; Gangavarapu, K.; Oliveira, G.; Robles-Sikisaka, R.; Rogers, T. F.; Beutler, N. A.; Burton, D. R.; Lewis-Ximenez, L. L.; de Jesus, J. G.; Giovanetti, M.; Hill, S. C.; Black, A.; Bedford, T.; Carroll, M. W.; Nunes, M.; Alcantara, L. C.; et al. Multiplex PCR Method for MinION and Illumina Sequencing of Zika and Other Virus Genomes Directly from Clinical Samples. *Nat. Protoc.* **2017**, *12*, 1261–1276.

(40) Zhu, Q.; Gao, Y.; Yu, B.; Ren, H.; Qiu, L.; Han, S.; Jin, W.; Jin, Q.; Mu, Y. Self-Priming Compartmentalization Digital LAMP for Point-of-Care. *Lab Chip* **2012**, *12*, 4755–4763.

(41) Yeh, E.-C.; Fu, C.-C.; Hu, L.; Thakur, R.; Feng, J.; Lee, L. P. Self-Powered Integrated Microfluidic Point-of-Care Low-Cost Enabling (SIMPLE) Chip. *Sci. Adv.* **2017**, *3*, No. e1501645.

(42) Zhou, S.; Gou, T.; Hu, J.; Wu, W.; Ding, X.; Fang, W.; Hu, Z.; Mu, Y. A Highly Integrated Real-Time Digital PCR Device for Accurate DNA Quantitative Analysis. *Biosens. Bioelectron.* **2019**, *128*, 151–158.

(43) Selck, D. A.; Ismagilov, R. F. Instrument for Real-Time Digital Nucleic Acid Amplification on Custom Microfluidic Devices. *PLoS One* **2016**, *11*, No. e0163060.

(44) Wang, J.; Ramakrishnan, R.; Tang, Z.; Fan, W.; Kluge, A.; Dowlati, A.; Jones, R. C.; Ma, P. C. Quantifying EGFR Alterations in the Lung Cancer Genome with Nanofluidic Digital PCR Arrays. *Clin. Chem.* **2010**, *56*, 623–632.

(45) Zhang, B.; Xu, C. W.; Shao, Y.; Wang, H. T.; Wu, Y. F.; Song, Y. Y.; Li, X. B.; Zhang, Z.; Wang, W. J.; Li, L. Q.; Cai, C. L. Comparison of Droplet Digital PCR and Conventional Quantitative PCR for Measuring EGFR Gene Mutation. *Exp. Ther. Med.* **2015**, *9*, 1383–1388.

(46) Watanabe, M.; Kawaguchi, T.; Isa, S. i.; Ando, M.; Tamiya, A.; Kubo, A.; Saka, H.; Takeo, S.; Adachi, H.; Tagawa, T.; Kakegawa, S.; Yamashita, M.; Kataoka, K.; Ichinose, Y.; Takeuchi, Y.; Sakamoto, K.; Matsumura, A.; Koh, Y. Ultra-Sensitive Detection of the Pretreatment EGFR T790M Mutation in Non-Small Cell Lung Cancer Patients with an EGFR-Activating Mutation Using Droplet Digital PCR. *Clin. Cancer Res.* **2015**, *21*, 3552–3560.

(47) Soria, J. C.; Ohe, Y.; Vansteenkiste, J.; Reungwetwattana, T.; Chewaskulyong, B.; Lee, K. H.; Dechaphunkul, A.; Imamura, F.; Nogami, N.; Kurata, T.; Okamoto, I.; Zhou, C.; Cho, B. C.; Cheng, Y.; Cho, E. K.; Voon, P. J.; Planchard, D.; Su, W. C.; Gray, J. E.; Lee, S. M.; et al. Osimertinib in Untreated EGFR-Mutated Advanced Non-Small-Cell Lung Cancer. *N. Engl. J. Med.* **2018**, *378*, 113–125.

(48) Costa, D. B. Kinase Inhibitor-Responsive Genotypes in EGFR Mutated Lung Adenocarcinomas: Moving Past Common Point Mutations or Indels into Uncommon Kinase Domain Duplications and Rearrangements. *Transl. Lung Cancer Res.* **2016**, *5*, 331–337.

(49) Zhou, W. J.; Ercan, D.; Chen, L.; Yun, C. H.; Li, D. N.; Capelletti, M.; Cortot, A. B.; Chiriac, L.; Iacob, R. E.; Padera, R.; Engen, J. R.; Wong, K. K.; Eck, M. J.; Gray, N. S.; Janne, P. A. Novel Mutant-Selective EGFR Kinase Inhibitors against EGFR T790M. *Nature* **2009**, *462*, 1070–1074.

(50) Oxnard, G. R.; Paweletz, C. P.; Kuang, Y. A.; Mach, S. L.; O'Connell, A.; Messineo, M. M.; Luke, J. J.; Butaney, M.; Kirschmeier, P.; Jackman, D. M.; Janne, P. A. Noninvasive Detection of Response and Resistance in EGFR-Mutant Lung Cancer Using Quantitative Next-Generation Genotyping of Cell-Free Plasma DNA. *Clin. Cancer Res.* **2014**, *20*, 1698–1705.

(51) Wang, Z. J.; Chen, R.; Wang, S. H.; Zhong, J.; Wu, M. N.; Zhao, J.; Duan, J. C.; Zhuo, M. L.; An, T. T.; Wang, Y. Y.; Bai, H.; Wang, J. Quantification and Dynamic Monitoring of EGFR T790M in Plasma Cell-Free DNA by Digital PCR for Prognosis of EGFR-TKI Treatment in Advanced NSCLC. *PLoS One* **2014**, *9*, No. e110780.

(52) Yin, J.; Suo, Y.; Zou, Z.; Sun, J.; Zhang, S.; Wang, B.; Xu, Y.; Darland, D.; Zhao, J. X.; Mu, Y. Integrated Microfluidic Systems with Sample Preparation and Nucleic Acid Amplification. *Lab Chip* **2019**, *19*, 2769–2785.

(53) Lobato, I. M.; O'Sullivan, C. K. Recombinase Polymerase Amplification: Basics, Applications and Recent Advances. *TrAC, Trends Anal. Chem.* **2018**, *98*, 19–35.

(54) Chen, J.; Xu, Y.; Yan, H.; Zhu, Y.; Wang, L.; Zhang, Y.; Lu, Y.; Xing, W. Sensitive and Rapid Detection of Pathogenic Bacteria from Urine Samples Using Multiplex Recombinase Polymerase Amplification. *Lab Chip* **2018**, *18*, 2441–2452.

(55) Shin, Y.; Perera, A. P.; Kim, K. W.; Park, M. K. Real-Time, label-free isothermal solid-phase amplification/detection (ISAD) device for rapid detection of genetic alteration in cancers. *Lab Chip* **2013**, *13*, 2106–2114.

(56) Song, J. Z.; Mauk, M. G.; Hackett, B. A.; Cherry, S.; Bau, H. H.; Liu, C. C. Instrument-Free Point-of-Care Molecular Detection of Zika Virus. *Anal. Chem.* **2016**, *88*, 7289–7294.

(57) Hongwarittorn, I.; Chaichanawongsaroj, N.; Laiwattanapaisal, W. Semi-Quantitative Visual Detection of Loop Mediated Isothermal Amplification (LAMP)-Generated DNA by Distance-Based Measurement on a Paper Device. *Talanta* **2017**, *175*, 135–142.

(58) Tomita, N.; Mori, Y.; Kanda, H.; Notomi, T. Loop-Mediated Isothermal Amplification (LAMP) of Gene Sequences and Simple Visual Detection of Products. *Nat. Protoc.* **2008**, *3*, 877.

(59) Kreutz, J. E.; Wang, J. S.; Sheen, A. M.; Thompson, A. M.; Staheli, J. P.; Dyen, M. R.; Feng, Q. H.; Chiu, D. T. Self-Digitization chip for Quantitative Detection of Human Papillomavirus Gene using Digital LAMP. *Lab Chip* **2019**, *19*, 1035–1040.

(60) Chang, H. C.; Chao, Y. T.; Yen, J. Y.; Yu, Y. L.; Lee, C. N.; Ho, B. C.; Liu, K. C.; Fang, J. U.; Lin, C. W.; Lee, J. H. A Turbidity Test Based Centrifugal Microfluidics Diagnostic System for Simultaneous Detection of HBV, HCV, and CMV. *Adv. Mater. Sci. Eng.* **2015**, *2015*, 8.